Investigating the Proton Transferring Route in a Heteroaromatic Compound Part I: A Trial to Develop Di- and Trifunctional Benzimidazole Model Compounds Inducing the Molecular Packing Structure with a Hydrogen Bond Network

Puripong Totsatitpaisan,[†] Kohji Tashiro,[‡] and Suwabun Chirachanchai*[,†]

The Petroleum and Petrochemical College, Chulalongkorn University, Soi Chula 12, Phyathai Rd., Pathumwan, Bangkok 10330, Thailand; and Department of Future Industry-oriented Basic Science and Materials, Graduate School of Engineering, Toyota Technological Institute, Hisakata 2-12-1, Tempaku, Nagoya 468-8511, Japan

Received: May 23, 2008; Revised Manuscript Received: July 31, 2008

Di- and trifunctional benzimidazole molecules, **1** and **2**, have been synthesized as the model compounds to identify their molecular packing structure and hydrogen bond network, which is possibly involved in the proton transfer system belonging to its heteroaromatic functional groups. By carrying out the simple reaction between acid chloride and diamine, the desired benzimidazole model compounds are obtained with high yield above 60%. The comparison studies between the model compounds and benzimidazole reveal that the model compounds show well-packing structure with intermolecular hydrogen bonds similar to those observed in benzimidazole. The presence of solvent with **2** leads to the unique intermolecular hydrogen bonds between one molecule of **2** and six molecules of solvent (i.e., 2-propanol) resulting in the solvent-assisted intramolecular hydrogen bond network among benzimidazole functional groups. The comparative studies of the effect of temperature on the packing structure and hydrogen bond in the model compounds indicate that the development of the benzimidazole unit from monofunctional to difunctional and finally trifunctional enhances the intermolecular interaction between the molecules and results in the stronger molecular packing structure of the compounds. A study on proton conductivity by preparing the sulfonated poly(ether ether ketone) (SPEEK) membranes with benzimidazole, **1**, and **2** for 15 phr equivalent to benzimidazole group clarifies (i) incorporation of benzimidazole compounds improves the proton conductivity of SPEEK in dry condition and (ii) the increase in proton conductivity is relevant to the number of benzimidazole group on molecule.

Introduction

Proton transfer in hydrated perfluorosulphonic acid polymer is recognized as a key mechanism in the polymer electrolyte membrane fuel cell (PEMFC).[1−3] The proton conduction occurs through the hydrogen bonds between water molecules (hydranium ion) and sulfonate groups formed along the hydrophilic cluster channel. As the path way of hydranium ion is random,[4,5] the enhancement of proton conductivity has to rely on specific conditions such as acid treatment, humidity, thermal acceleration of proton movement, and so forth. The operating condition at intermediate temperature (120−160 °C) is another requirement if we consider the activation of catalyst on electrodes.[6−9] Unfortunately, the consequent loss of water molecules in the membrane due to evaporation above 80 °C and the cost of the commercially available membrane, Nafion, limit the usage of the PEMFC.[3,10] Recently, an alternative system of the polymer electrolyte membrane has been introduced based on the mechanism of proton transfer in a water-free condition. In this system, the function of heterocyclic compounds, especially imidazole, benzimidazole, and pyrazole, was proposed to play a role as the proton carrier in a dry system even at high temperature via a mechanism involving proton transfer- and reorientation processes.[11−14] By considering this proton transfer mechanism, the regularity on molecular arrangement of the heterocycles is essential. However, most of the studies on these materials are about the incorporation of heterocyclic moieties in the main chain,[10,15,16] side chain,[17−19] or as the filler mixed in polymer matrix.[20−22] An effective proton transferring route is still needed to be clarified in detail to understand how to overcome the low mobility of heteroaromatic groups and solve the lack of molecular arrangement of proton carrier parts.

In order to obtain an effective proton transfer property, the proton conducting mechanism has to be favored by developing a molecularly aligned system of heterocyclic compounds, which make the proton hopping occur easily. However, this kind of work is rarely reported. One possibility is to build up a well-defined proton transferring route based on the specific molecular arrangement. In the past, Barboiu's group showed the specific ion conducting pathways based on the self-assembly of hybrid organic−inorganic urea-based derivatives.[23,24] However, in order to apply those derivatives in the PEMFC, the severe operating conditions bringing in the oxidation, reduction together with temperature above 120 °C, and saturated humidity including impurities are the points to be considered.

On this viewpoint, the present work proposes the molecular design and synthesis of ethylene-1,2-di-2-benzimidazole, **1**, (difunctional benzimidazole) and benzene-1,3,5-tri-2-benzimidazole, **2**, (trifunctional benzimidazole) to be the model compounds inducing the formation of molecular packing structures that will further act as an effective proton transferring path. Compound **1** is attractive in terms of the greater number of proton carriers compared with a single benzimidazole, the symmetrical structure, and the possibly higher thermal stability, whereas compound **2** shows further advantages of the planar

* To whom correspondence should be addressed. Phone: 662-218-4154. Fax: 662-215-4459. E-mail: csuwabun@chula.ac.th.
[†] Chulalongkorn University.
[‡] Toyota Technological Institute.

10.1021/jp8045774 CCC: $40.75
Published on Web 09/25/2008

SCHEME 1: Synthesis of Ethylene-1,2-di-2-benzimidazole, 1

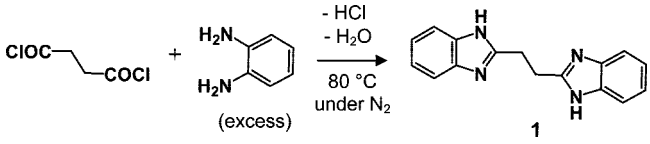

shape which might enhance the π-π stacking conformation, also the greater number of benzimidazole units, and higher thermal stability. The works also extend to an investigation about how the hydrogen bond networks formed in the materials including the change in packing structures and hydrogen bonds under the effects of solvent molecules and temperature as compared with a single benzimidazole compound. The structural investigation is successful on the basis of the simultaneous measurement of wide-angle X-ray diffraction (WAXD) and differential scanning calorimetric (DSC) analysis, temperature dependent Fourier transform infrared (FTIR) spectroscopy, and X-ray crystal structure analysis.

Experimental Section

Materials. Benzimidazole, 1,3,5-benzenetricarbonyltrichloride, and 1,2-phenylenediamine were purchased from Aldrich, Germany. Succinyl chloride was bought from Fluka, Switzerland. Poly(ether ether ketone) (PEEK) was a gift from JJ-Degussa Chemical (Thailand) Ltd., Thailand. All chemicals and solvents were analytical grade and were used without further purification.

Synthesis of 1. Compound **1** was synthesized as shown in Scheme 1. Succinyl chloride (1.30 g, 7.97×10^{-3} mol) in xylene (150 mL) was added dropwisely into a vigorously stirred solution of 1,2-phenylenediamine (2.66 g, 2.45×10^{-2} mol) in xylene (50 mL) at 80 °C under nitrogen atmosphere. The reaction was proceeded for 24 h yielding the dark green precipitates. The precipitates were collected and dissolved in methanol prior to reprecipitation by adding 1.0 M NaOH solution to obtain the purple precipitates. Characterization: FT-IR (cm^{-1}): 3450 (weak, N−H stretching); 3200−2500 (strong, hydrogen bonded N−H stretching); 1452 and 1436 (strong, skeleton vibration of benzimidazole ring); 746 (strong, aromatic C−H bending). ^{1}H NMR (DMSO-d_6): δ 7.50 (4H, d, Ar−H); 7.10 (4H, s, Ar−H); 3.20 (4H, s, CH_2). Mass spectrometry (*m/z*): 263.13. FW of $C_{16}H_{14}N_4$: 262. Elemental analysis (EA) (%) Found: C, 71.99; H, 5.70; N, 20.49. Calcd for $C_{27}H_{18}N_6$: C, 73.28; H, 5.34; N, 21.37.

Synthesis of 2. The steps of reaction are summarized in Scheme 2. 1,3,5-Benzenetricarbonyltrichloride (0.2310 g, 8.53×10^{-4} mol) in xylene (150 mL) was added dropwisely into a vigorously stirred solution of 1,2-phenylenediamine (0.3820 g, 3.51×10^{-3} mol) in xylene (50 mL) at 70 °C under nitrogen atmosphere. The red brownish precipitates were obtained after overnight. The precipitates were washed a few times with xylene before neutralization in methanol with 1.0 M NaOH solution to obtain green yellow solution. The solvent was changed from methanol to ethylene glycol, and the solution was refluxed at 150 °C under vacuum for 24 h to obtain yellow precipitates. The product was washed several times with distilled water and recrystallized in methanol to obtain a crystal of **2**. Single crystals necessary for X-ray structure analysis were prepared by further recrystallizing **2** in 2-propanol. Characterization: FT-IR (cm^{-1}): 3500−2800 (strong, hydrogen bonded N−H and O−H stretching); 1436 (strong, skeleton vibration of benzimidazole ring); 742 (strong, aromatic C−H bending). ^{1}H NMR (CD_3OD): δ 8.76 (3H, s, Ar−H (benzene)); 7.62 (6H, br, Ar−H (benzimidazole)); 7.24 −7.27 (6H, dd, Ar−H (benzimidazole)). Sublimed crystal of **2** was obtained from subliming **2** at 340 °C under reduced pressure. Characterization: FT-IR (cm^{-1}): 3430 (weak, N−H stretching); 3000−2200 (strong, hydrogen bonded N−H stretching); 1444 (strong, skeleton vibration of benzimidazole ring); 743 (strong, aromatic C−H bending). Mass spectrometry (*m/z*): 427.16. FW of $C_{27}H_{18}N_6$: 426. Elemental analysis (%) Found: C, 73.37; H, 4.91; N, 18.55. Calcd for $C_{27}H_{18}N_6$: C, 76.06; H, 4.23; N, 19.72.

SCHEME 2: Synthesis of Benzene-1,3,5-tri-2-benzimidazole, 2

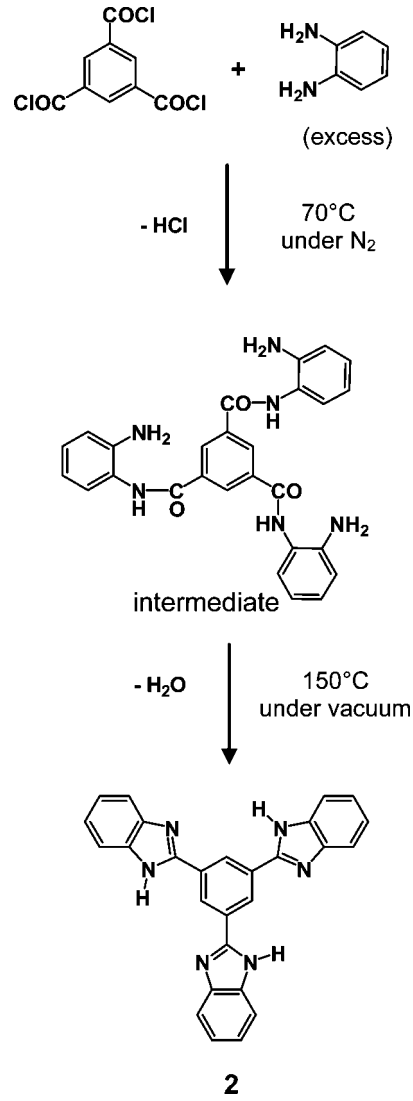

Sulfonation of PEEK. Sulfonated poly(ether ether ketone) (SPEEK) PEEK was prepared by modifying the sulfonation procedure reported by Gaowen et al.[25] In brief, PEEK powder (20 g) was dried in a vacuum oven at 100 °C overnight before dissolving in a liter of concentrated (98%) sulfuric acid (H_2SO_4) at room temperature under strong agitation for 48 h. The solution obtained was gradually reprecipitated in ice-cold water. The suspension was filtered and washed several times with distilled water until neutral pH. The precipitate was dried under vacuum at 100 °C for 12 h to obtain the SPEEK with 65% degree of sulfonation as an orange solid.

Instruments and Equipment. FT-IR spectra were recorded on a Thermo Nicolet Nexus 670 Fourier transform infrared spectrophotometer at a resolution of 2 cm^{-1} in the frequency

range 4000−400 cm^{-1}, using a deuterated triglycinesulfate detector (DTGS). Temperature-dependent FT-IR spectroscopy was performed with an in-house temperature-controlled sample holder. Proton nuclear magnetic resonance (^{1}H NMR) spectra were collected by a Varian Mercury-400BB spectrometer using tetramethylsilane as an internal standard and DMSO-d_6 and CD_3OD as solvents for **1** and **2**, respectively. Mass spectra were measured with a Bruker micrOTOF mass spectrometer (MS) in positive ion mode. Compound **1** was ionized by electrospray ionization (ESI), whereas **2** was ionized by atmospheric pressure chemical ionization (APCI) interface operated at 250 °C under an electrical field strength of 4 kV. Thermal analyses were performed with a TA Instrument Q-1000 DSC analyzer scanning from 25 to 500 °C at a heating/cooling rate of 10 °C/min under nitrogen atmosphere. Elemental analyses were performed by a Bruker 2000 series III CHNO/S analyzer. Simultaneous wide-angle X-ray diffraction (WAXD) measurement and DSC analysis were done by using a Rigaku X-ray diffractomer/RINT-TTR III Thermo plus DSC analyzer in the temperature range from 25 to 150 °C at a heating/cooling rate of 3 °C/min under nitrogen atmosphere. X-ray single crystal structure analysis was carried out by a Rigaku R-AXIS RAPID-II diffractometer with graphite-monochromated Mo Kα radiation at 296 K. The structure was solved by direct method (SIR92)[26] and refined by the full matrix least-squares procedures on $|F|^2$ (F: structure factor). All non-hydrogen atoms were refined for anisotropic thermal parameters as well as the fractional coordinates. All the analyses were performed using the "Crystal Structure" software package.[26] Proton conductivities were analyzed by an AC impedance spectrometer using an IM6 Zahner Elektrik connected to a PC running electrochemical impedance software in the frequency range $10-10^6$ Hz at 80−120 °C under the dried condition. In-house stainless steel sealed-off cells connected in series were applied.

Proton Conductivity Measurement. Benzimidazole, **1**, and sublimed **2** were dissolved in DMSO before mixing with SPEEK/DMSO solution under the content of 15 phr equivalent to the benzimidazole group and casted to obtain SPEEK-1BI, SPEEK-2BI, and SPEEK-3BI, respectively. The pure SPEEK membrane was similarly prepared without adding benzimidazole compounds and was used as a reference. The membranes for 5−6 layers were stacked (thickness ∼400 μm) and assembled into the impedance test cells, which were connected in series by stainless tubes. All of the cells were purged by dry nitrogen for more than 2 h to ensure the low humidification. The measurements were carried out in the frequency range $10-10^6$ Hz at 80−120 °C under the continuous dry nitrogen gas flow at 10 mL/min. The proton conductivities were calculated from the impedances estimated at phase angle zero.

Results and Discussion

Synthesis of Difunctional Benzimidazole Compound. Persson et al.[7a] reported a single step reaction to obtain benzimidazole compound from poly(ethylene glycol) bis(carboxymethyl) ether and 1,2-phenylenediamine. However, after several attempts to prepare **1** from the reaction between succinic acid and phenylenediamine using similar conditions, we found that the expected difunctional benzimidazole derivative is difficult to be obtained. Therefore, we changed from dicarboxylic acid to diacid chloride (i.e., succinyl chloride), which has stronger reactivity to diamine than that of carboxylic acid. The reaction took place at 80 °C under nitrogen atmosphere for 24 h, as shown in Scheme 1. An excess amount of phenylenediamine together with the slow addition of dilute succinyl chloride solution into the concentrated phenylendiamine solution were done to suppress the polymerization reaction between the two reagents. After the reaction finished, purification was done by dissolving the crude product in methanol before adding NaOH into the solution to reprecipitate the final product. The difunctional benzimidazole, **1**, was obtained as purple powder. This one-pot synthesis was found to be an easy and efficient condition to prepare **1** with the 63.6% yield.

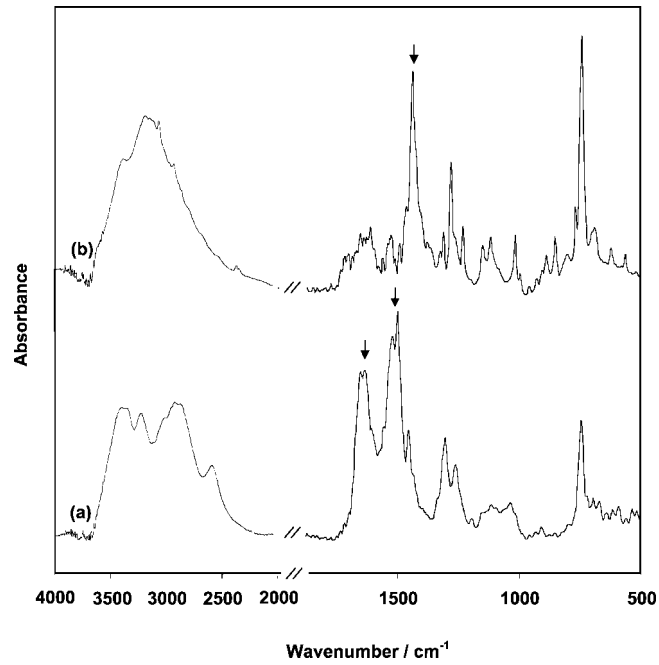

Figure 1. FT-IR spectra of intermediate compound (a) and $\mathbf{2}_{recryst}$ (b).

The success of preparation of **1** was confirmed by FT-IR, ^{1}H NMR, MS, and EA. The FT-IR spectrum of **1** shows the important peaks of N−H stretching at 3450 cm^{-1}, hydrogen bonded N−H stretching of the benzimidazole unit at 3200−2500 cm^{-1}, skeleton vibration of the benzimidazole ring at 1452 and 1436 cm^{-1}, and C−H bending of the aromatic at 746 cm^{-1}. The ^{1}H NMR spectrum indicates the peaks related to **1** at 7.50, 7.10, and 3.20 ppm, which correspond to the protons at the Ar−H position in the benzimidazole ring and the ones at the CH_2 position, respectively. The ESI-MS spectrum reveals the parent peaks at $m/z = 263.13$ and 285.43, which represent the molecular weight of **1** with proton and with sodium ion, respectively (formula weight of **1** = 262). The CHN analysis result also supports the successful preparation condition of **1**.

Synthesis of Triifunctional Benzimidazole Compound, 2. In contrast with the synthesis of **1**, we found that **2** is difficult to prepare by the single step reaction. Although, the condition was adjusted, only the amide derivatives were obtained. Thus, we modified the synthesis condition by separating into two steps (i) amidation and (ii) ring closure, as shown in Scheme 2. In the first step, after triacid chloride was reacted with the diamine, red brownish precipitates were obtained. The precipitates show the characteristic peaks of an amide bond: C═O (amide I) at 1650 cm^{-1} and N−H (amide II) at 1521 cm^{-1} (Figure 1a). Although, not yet confirmed the obtain of trifuntional amide intermediate was obtained at this step, the neutralization of protonated amines by NaOH was applied to recover the nucleophilicity of the amino groups for the cyclization in the next step. The amount of NaOH solution is important, since an insufficient amount causes a lower extent of cyclization while an excess one induces the cleavage of amide bond via a

sponification. However, the equivalent point for neutralization could be easily determined from the change in color of the methanol solution of the intermediate from brown to green (pH ~6.0). In the second step, the ring closure was done in ethylene glycol to obtain the trifunctional benzimidazole compound, **2**, by refluxing at 150 °C under reduced pressure. This step also initiates byproduct (i.e., water). The product was precipitated out from the solution and further collected as a yellow precipitates. After purification, the yellow needle crystals of **2**, which we termed as $\mathbf{2}_{recryst}$, was obtained from the methanol solution at room temperature (yield ~69%).

Figure 1b shows the disappearance of the peaks corresponding to amide bonds of the intermediate compound confirming the complete benzimidazole ring formation. The presence of a new band at 1436 cm^{-1} implies the skeletal vibration of benzimidazole ring. For ^1H NMR, the spectrum showed the peaks at 8.76, 7.62, and 7.33 ppm representing the protons at the center benzene ring and protons on the benzimidazole unit, respectively. The electrospray-TOF MS revealed the parent peak ($M + H^+$) at $m/z = 427.16$ corresponding to the molecular weight of **2** ($C_{27}H_{18}N_6$: FW = 426). Moreover, the EA result also supports the structure of **2** with the observed data :C, 73.37%; H, 4.91%; N, 18.55% (calculated value for $C_{27}H_{18}N_6$: C, 76.06%; H, 4.23%; N, 19.72%). It should be noted here that the incorporation of solvents in the crystal lattice of the compound might influence the accuracy of the CHN results of **1** and **2** (see crystal structure of $\mathbf{2}_{recryst}$ in Investigation of Molecular Packing Structures and Hydrogen Bonds in the Compounds section). All the results indicate that the synthesis condition is effective for three benzimidazole ring cyclization with high selectivity.

Investigation of Molecular Packing Structures and Hydrogen Bonds in the Compounds. On the basis of the viewpoint of the proton hopping mechanism in the PEMFC, the molecular packing and hydrogen bond network in the compound are important. Here, a series of benzimidazole-based structures was considered. The number of benzimidazole units together with the planar shape of the molecule are expected to induce the intermolecular interaction and result in developing molecular packing structure governed by the hydrogen bond network, which will offer an effective proton transfer mechanism between the molecules. X-ray crystal structure analysis is a useful technique to provide us a concrete structure related to the molecular packing structure and hydrogen bond network formation in the compound. However, when obtaining a single crystal is difficult, combined investigations of WAXD profile and the hydrogen bond pattern observed in FT-IR spectra gives us useful information.

In the first step, the studies on packing structure and hydrogen bond network formation of benzimidazole were studied to obtain reference information. The single crystal of benzimidazole was prepared by sublimation at 140 °C in vacuo and analyzed by performing X-ray crystal structure analysis. Figure 2 shows that the crystal is belonging to an orthorhombic system under Pccn with eight molecules in each unit cell. This structure is different from the ones obtained from the solution or melt growth crystals reported previously with $Pna2_1$ and four molecules in the unit cell.[27,28] The crystal structure reveals that the packing of benzimidazole molecules is formed with a one-dimensional hydrogen bond network. The NH···N distance of the intermolecular hydrogen bond between the adjacent molecules is about 2.8 Å, indicating a strong hydrogen bond interaction.[26]

As **1** does not give a single crystal, the X-ray crystal analysis was possible for only **2**. However, the transparent single crystal

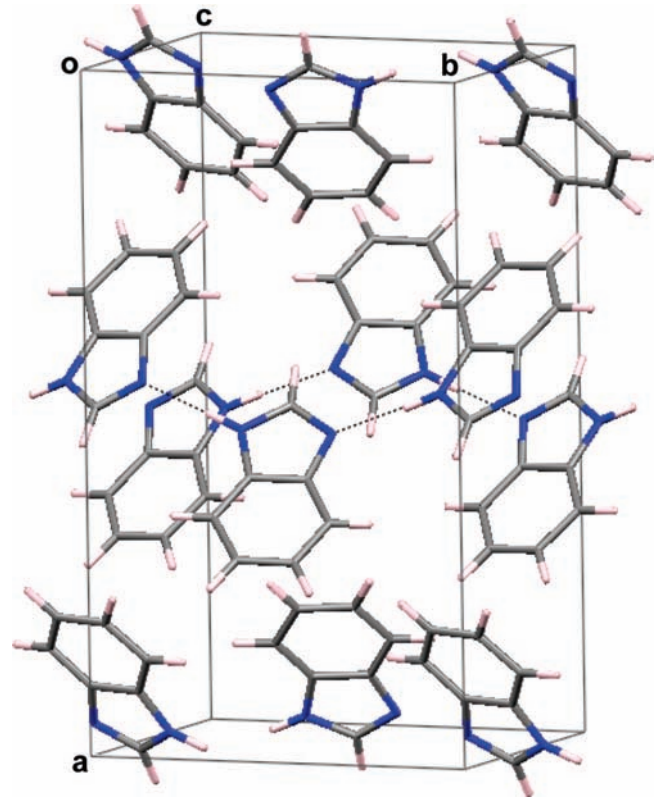

Figure 2. Crystal structure of benzimidazole prepared by sublimation. Crystal system: orthorhombic (Pccn); $a = 16.6754$ Å, $b = 9.7372$ Å, $c = 7.6219$ Å; $\alpha = \beta = \gamma = 90°$; $V = 1237.6$.

2, $\mathbf{2}_{recryst}$, obtained from recrystallizing **2** in 2-propanol solution was found to be unstable as it changed to be a turbid crystal after exposure in air for a while. This made the crystal become difficult for analysis. Figure 3 shows concrete 2D-XRD evidence from the crystalline (Figure 3a) becoming a mosaic aggregation of small crystals (Figure 3b) during air exposure, which may occur due to solvent evaporation. An attempt to obtain X-ray diffraction was carried out by immersing a single crystal of **2** in a glass capillary filled with isopropanol to overcome the solvent instability in the crystal lattice.

Figure 4a illustrates the crystal structure of **2** with 2-propanol. The structure analysis supports the success of our synthesis trifunctional benzimidazole compound. As expected, **2** coexists with 2-propanol in a unit cell under a structure of two molecules of **2** and twelve molecules of 2-propanol. This triangular molecule is surrounded by its solvent molecules. The conformation of **2** is not a complete planar (i.e., the three benzimidazole rings are slightly out of the plane of the core benzene). The conformational disorder of 2-propanol molecules might be due to their thermal vibration in the crystal, making the structure analysis be difficult to fix the position of 2-propanol in the crystal lattice as seen from the wide probability of carbon atomic position of 2-propanol in Figure 4b. This conformational disorder of solvent also brought limitation to the R value ~13% (without adding H).

The existence of hydrogen bonds between the nitrogen atoms of **2** and the oxygen atoms of the nearest 2-propanol molecules was observed with the N−H···O or N···H−O distances ~2.8 Å[26] (Figure 4a). These hydrogen bonds may result in the nonplanar conformation of **2** and might help the stabilization of the packing structure of **2** in the crystal lattice. Another type of hydrogen bond, O−H···O, is also extracted between the solvent molecules in the adjacent position. This leads to a unique

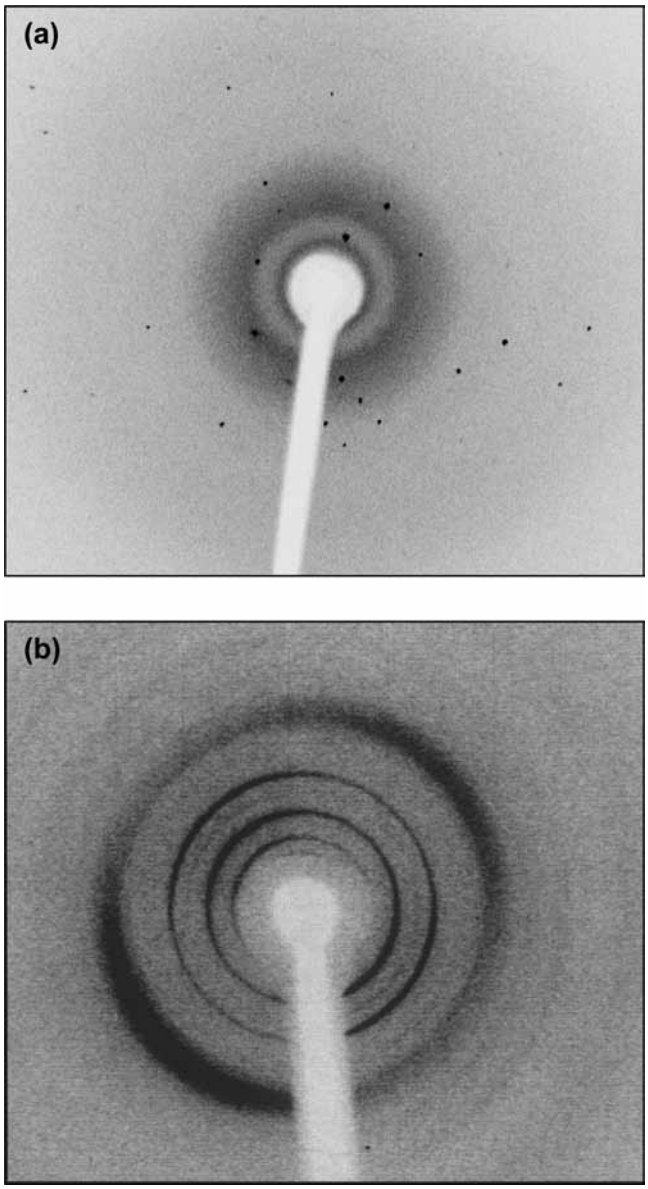

Figure 3. 2D X-ray diffraction image of crystal $\mathbf{2}_{recryst}$: transparent single crystal (a) and turbid crystal (b).

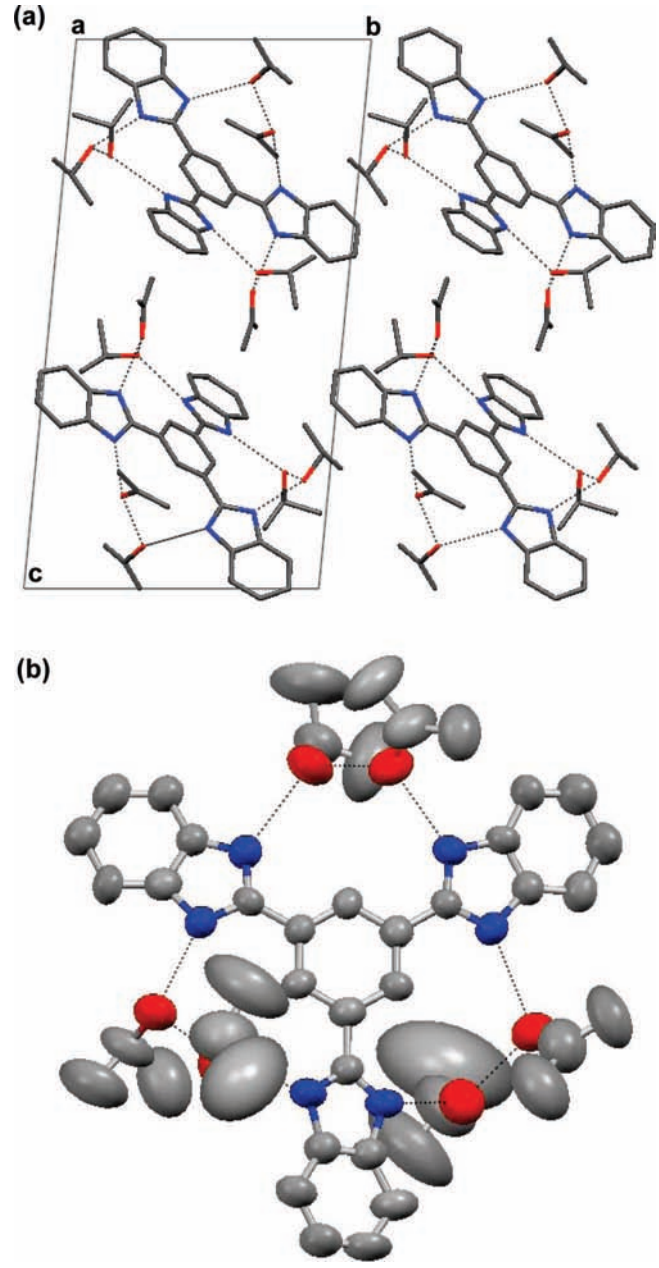

Figure 4. Crystal structure of **2** with 2-propanol ($\mathbf{2}_{recryst}$): overview of the hydrogen bond network between **2** and 2-propanol (a) and solvent-assisted intramolecular hydrogen bond network of **2** (b). Crystal system: triclinic ($P\bar{1}$); $a = 9.081$ Å, $b = 11.991$ Å, $c = 22.376$ Å; $\alpha = 95.134°$, $\beta = 93.043°$, $\gamma = 95.515°$; $V = 2394.2$.

characteristic of the intermolecular hydrogen bond network between one molecule of **2** and six molecules of 2-propanol resulting in the "solvent-assisted intramolecular hydrogen bond network" among benzimidazole functional groups in **2**. This structure is expected to offer a proton transferring pathway among all three benzimidazole groups in **2** (Figure 4b). But, the complex of **2** with solvent molecules might not be preferable for proton conductive initiation, which requires the intermolecular hydrogen bond network. Moreover, the packing structure of **2** in a solvent-free condition is an ideal case for proton hopping in high operating temperature. Therefore, the crystal **2** without solvent incorporated, which we termed as $\mathbf{2}_{sublim}$, was acquired by subliming **2** at 340 °C in vacuo. At present, the preparation and investigation of a single crystal of $\mathbf{2}_{sublim}$ by single crystal structure analysis is under progress. Here, molecular packing structure and hydrogen bond formation of $\mathbf{2}_{sublim}$ based on FT-IR, WAXD including temperature-dependent analyses were focused.

Figure 5 shows the comparative FT-IR spectra of **1** (b), $\mathbf{2}_{recryst}$ (c), and $\mathbf{2}_{sublim}$ (d) as compared to that of benzimidazole (a). It is important to note that benzimidazole shows the characteristic bands in the wide region of 3250−2500 cm^{-1} (Figure 5a), which can be assigned to the strong N−H···N intermolecular hydrogen bonds network as illustrated in its crystal structure result.[24] Comparing **1** with benzimidazole, the characteristic peaks representing N−H···N hydrogen bonds are also observed at 3100−2500 cm^{-1} (Figure 5b). Therefore, it is reasonable to expect the formation of an intermolecular hydrogen bond in **1**. In the case of $\mathbf{2}_{recryst}$, the hydrogen bond pattern and position are different from those of benzimidazole. This reflects the presence of 2-propanol in the crystal, which generates the O−H···O or O−H···N type hydrogen bond resulting in the broad peak in the O−H stretching region, 3600−2500 cm^{-1} (Figure 5c). The hydrogen bond with 2-propanol is strongly supported by the changes in position and pattern of this characteristic band from 3600−2500 cm^{-1} to 3100−2200 cm^{-1} (Figure 5c and d) as compared $\mathbf{2}_{recryst}$ with $\mathbf{2}_{sublim}$. The similar

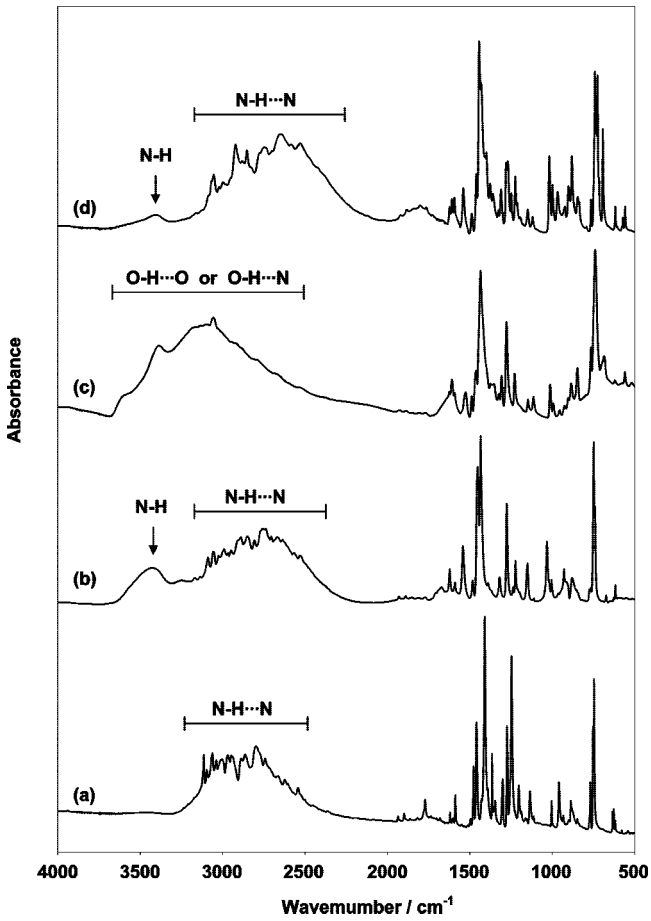

Figure 5. FT-IR spectra of benzimidazole (a), **1** (b), $\mathbf{2}_{recryst}$ (c), and $\mathbf{2}_{sublim}$ (d).

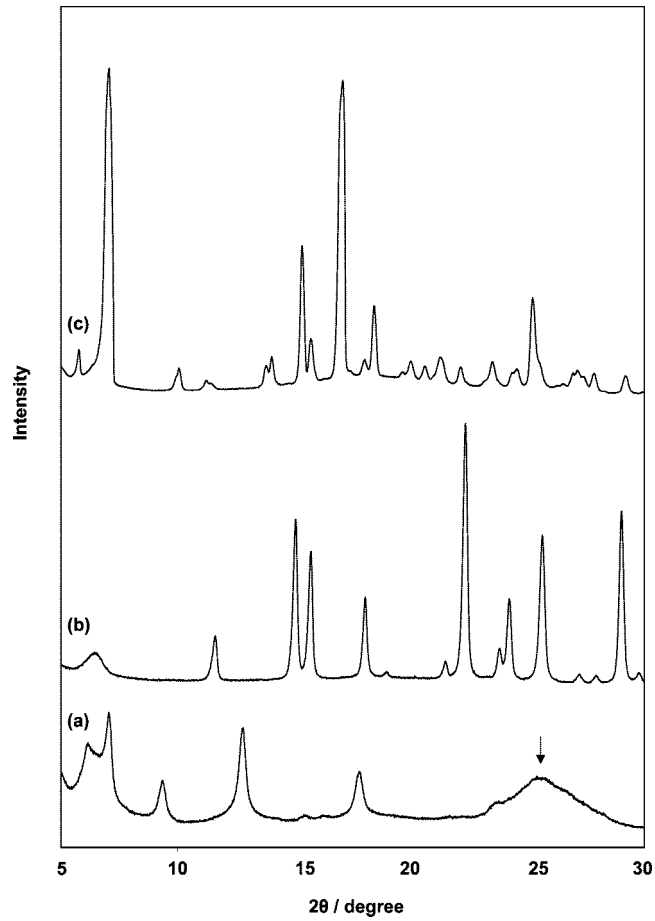

Figure 6. WAXD patterns of a turbid crystal $\mathbf{2}_{recryst}$ (a), **1** (b), and $\mathbf{2}_{sublim}$ (c).

peaks and patterns related to hydrogen bond formation of **1**, $\mathbf{2}_{sublim}$, and benzimidazole support our expectation of intermolecular hydrogen bond formation in **1** and **2** without solvent.

Molecular packing of the compounds was studied by WAXD. Figure 6 shows the WAXD patterns of a turbid crystal of $\mathbf{2}_{recryst}$ (a), **1** (b), and $\mathbf{2}_{sublim}$ (c). It is important to note that the turbid crystal of $\mathbf{2}_{recryst}$, which was obtained after leaving the single crystal in the air for a while, should remain some regularities in packing structure as the WAXD profile of this crystal shows sharp peaks with a single broad peak at 25.5° 2θ. For **1** and $\mathbf{2}_{sublim}$, the sharp peaks in all 2θ are observed. This indicates that the molecules of **1** and $\mathbf{2}_{sublim}$ were in well-packing structure as well.

Moreover, the DSC analyses reveal that **1** and **2** are high thermally stable compounds. For **1**, the degradation temperature was found at 429 °C without any melting temperature (T_m). This also reflects the strong intermolecular hydrogen bond between the molecules as discussed in the FT-IR spectrum. On the other hand, **2** was stable up to 500 °C with T_m and crystallization temperature (T_c) at 445 and 398 °C, respectively (Figure 7). An endothermic peak at 119 °C in the first heating cycle represents evaporation of 2-propanol molecules. The fact that the release of 2-propanol is at 119 °C, which is much higher than its boiling point (82 °C), indicates the incorporation of solvent in the crystal lattice, and as a result, the higher energy is required for its evaporation. The disappearance of this band in the second heating cycle suggests that 2-propanol was released completely in the prior cycle. This supports the crystal structure of $\mathbf{2}_{recryst}$ (Figure 4). The shifts of T_m and T_c in the second heating−cooling cycle as compared to the first cycle imply the different molecular packing structure between these two cycles as consequences of solvent exclusion and thermal treatment.

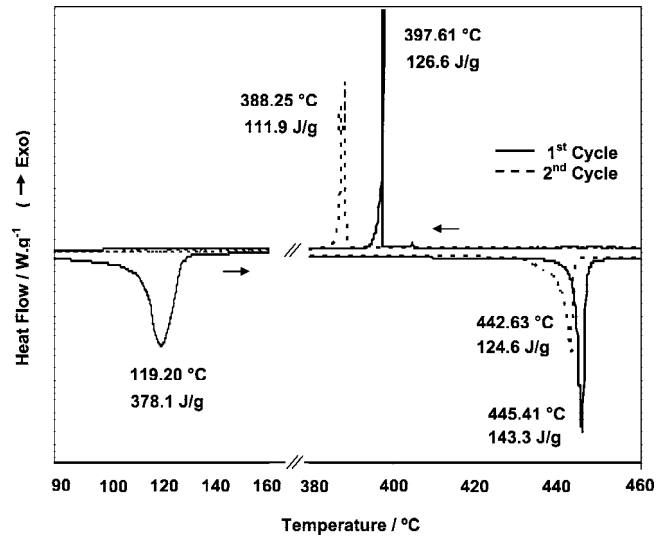

Figure 7. DSC thermogram of $\mathbf{2}_{recryst}$: first heating−cooling cycle (—) and second heating−cooling cycle (---).

Combining all the results, although the precise structure of $\mathbf{2}_{sublim}$ from single crystal analysis is still under investigation, the information from FT-IR, WAXD, and DSC lead to a conclusion of the well-packing structure with strong intermolecular hydrogen bonds in both **1** and $\mathbf{2}_{sublim}$ as seen in the case of benzimidazole.

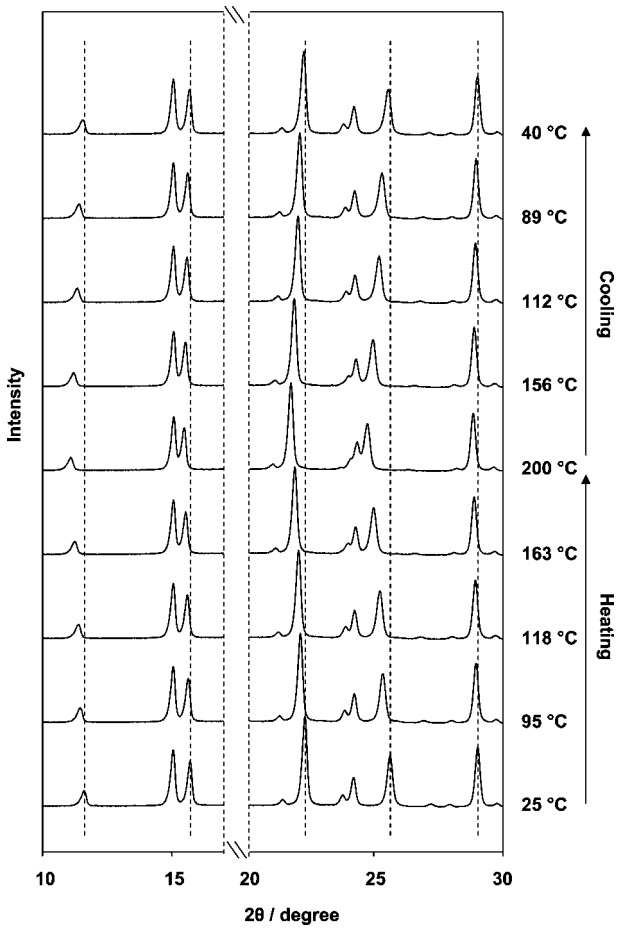

Figure 8. WAXD patterns of **1** at various temperatures.

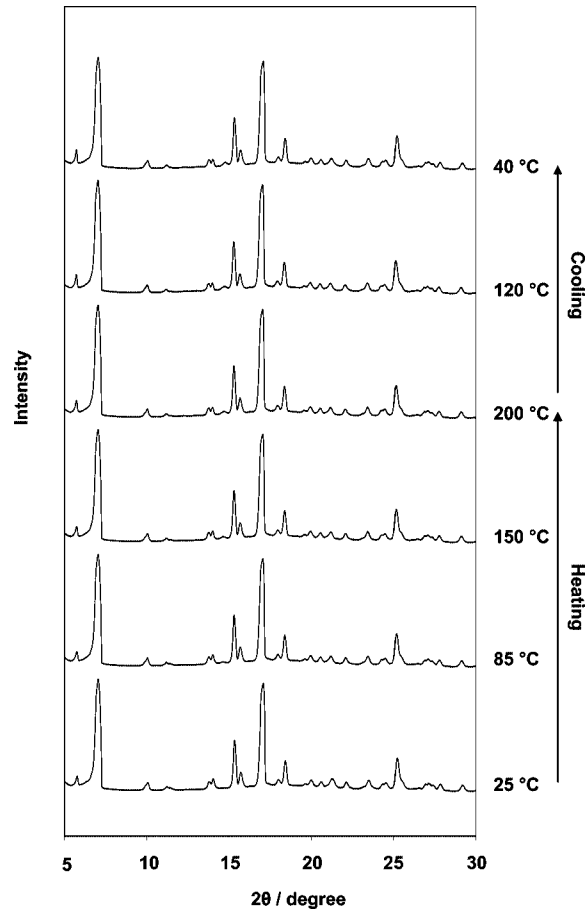

Figure 9. WAXD patterns of $\mathbf{2}_{\text{sublim}}$ at various temperatures.

Temperature Dependency of Molecular Packing Structure and Hydrogen Bond Network. Thermal acceleration of proton movement is a key factor to favor the proton transfer mechanism of the PEMFC. Therefore, it is essential to study how molecular arrangement and the hydrogen bond formation are related to the temperature. Simultaneous WAXD-DSC measurements at a temperature range from 25 to 200 °C under nitrogen atmosphere were carried out. As shown in Figure 8, the WAXD patterns of **1** show that the peaks shift (i.e., 11.6°, 15.7°, 22.3°, and 25.6° 2θ) to a lower angle when heating up and shift back to the former positions when cooling down. It is important to note that at the same time, the DSC analysis of the compound showed neither endo- nor exothermic peaks during heating and cooling. This implied that the packing structure of **1** was undergone thermal expansion when the temperature increased and contraction when the temperature decreased.

For $\mathbf{2}_{\text{sublim}}$, there is no change of WAXD profiles under heating and cooling in this temperature range (Figure 9) and also no peak identified in the DSC thermogram. This suggests that the packing structure of **2** when there is no solvent might be tighter than that of **1**. The thermal energy in this temperature range might not be enough to initiate the molecular movement. This supports our expectation about the more effective molecular interaction in $\mathbf{2}_{\text{sublim}}$ than that of **1** based on the greater number of hydrogen bonds and the π-π interactions derived by the planar shape structure.

The temperature dependency studies were extended to the hydrogen bond analysis using FT-IR spectroscopy. The measurements were carried out using an in-house sample holder, which can control the temperature in the range 25−250 °C. Figure 10 shows the FT-IR patterns of benzimidazole, **1**,and $\mathbf{2}_{\text{sublim}}$. As all samples show no significant change in fingerprint region, 1600−500 cm^{-1}, only the region of 3600−2200 cm^{-1} is shown for discussion. For benzimidazole (Figure 10a), the intensity of the peaks at 3030−2500 cm^{-1} decreases gradually when the sample was heated from room temperature to 160 °C. When benzimidazole was heated, the well-packed molecules might be vibrated and moved apart for some distance and resulted in the change of the intermolecular hydrogen bond from the strong interaction to the weaker one. This initiates the decrease in peak intensity related to strong hydrogen bonded N−H stretching (3030−2500 cm^{-1}) and increase in peak intensity corresponded to weaker hydrogen bonded N−H stretching (3100−3030 cm^{-1}). Here, Scheme 3a illustrates a simplified N−H···N hydrogen bond network as observed in the crystal structure of benzimidazole and the speculated changes of molecular packing structure responding to thermal treatment. It should be noted that the peaks disappeared when benzimidazole was heated over its melting point (171 °C). Similar to the case of benzimidazole, Figure 10b and c shows that the changes in peak intensity related to bonded N−H stretching of **1** and $\mathbf{2}_{\text{sublim}}$ are in the same tendency under heating from room temperature to 250 °C. This change is reversible when the samples were cooled to room temperature reflecting the stable molecular packing structure in this temperature range. For **1** (Figure 10b), as mentioned above (see the Investigation of Molecular Packing Structures and Hydrogen Bonds in the Compounds section), the WAXD-DSC result suggests the thermal expansion of the molecular packing structure of the compound under an increase of temperature (Figure 8). This corresponds to the changes in FT-IR peak intensity from the

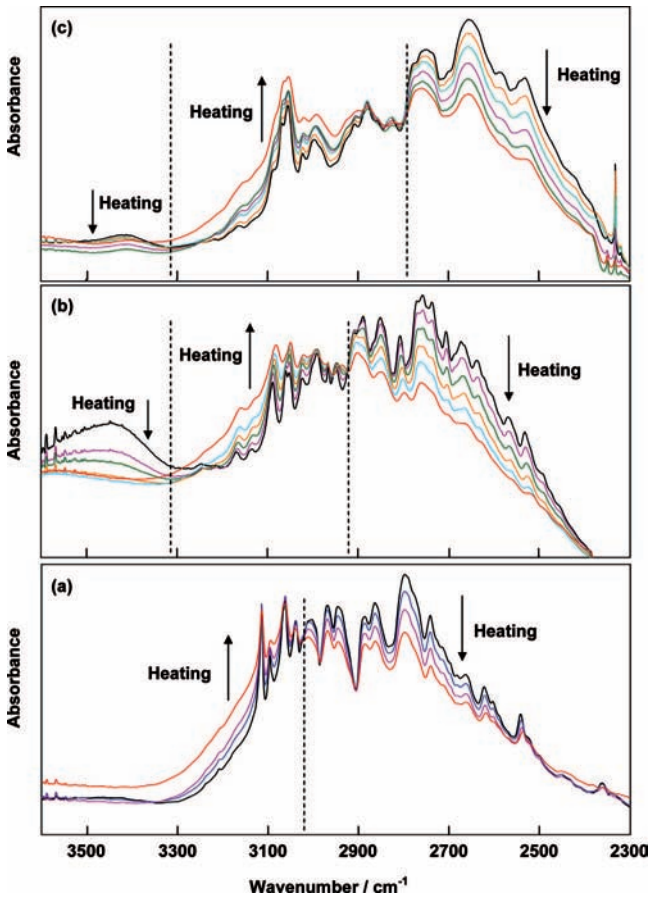

Figure 10. Temperature-dependent FT-IR spectra: benzimidazole (a), **1** (b), and $\mathbf{2}_{\text{sublim}}$ (c).

region regarding to strong hydrogen bonds (2930−2510 cm^{-1}) to weaker hydrogen bonds (3230−2930 cm^{-1}). The molecules are apart under thermal expansion as illustrated in Scheme 3b. The broad peak and the decrease in peak intensities at 3450 cm^{-1} under the heating step indicates the presence of some weak bonded N−H stretching. In the case of $\mathbf{2}_{\text{sublim}}$ (Figure 10c), although the simultaneous WAXD-DSC measurement shows no change in molecular packing structure, the FT-IR spectra show the similar decrease in peak intensity related to strong hydrogen bonded N−H (2810−2370 cm^{-1}) and increase in peak intensity belonged to weaker hydrogen bond N−H (3200−2810 cm^{-1}). This suggests to us that **2** might vibrate either in-plane or out-of-plane to result in the change from strong hydrogen bond to weaker hydrogen bond, as shown in Scheme 3c. It should be noted that when we compare the peak positions at 3030, 2930, and 2810 cm^{-1} of benzimidazole, **1**, and $\mathbf{2}_{\text{sublim}}$, respectively, we speculate that the strength of hydrogen bond interactions is in the order of benzimidazole < **1** < **2**. In other words, **2** retains the changes of the stronger bonded N−H stretching peaks than **1** whereas benzimidazole hardly maintains its hydrogen bond during the heat. This can be explained by the fact that **1** contains a greater number of benzimidazole units than benzimidazole, which allows more possibilities of intermolecular hydrogen bonds between the molecules. For **2**, the molecule is stiff and bulky with planar shape to obstruct the side-by-side hydrogen bond formation as observed in the case of benzimidazole. Therefore, we speculated that the molecular packing structure should be derived by a stacking conformation, as demonstrated in Scheme 3c. This structure reflects the stronger intermolecular interaction of **2** than that of **1**, under the same temperature effect.

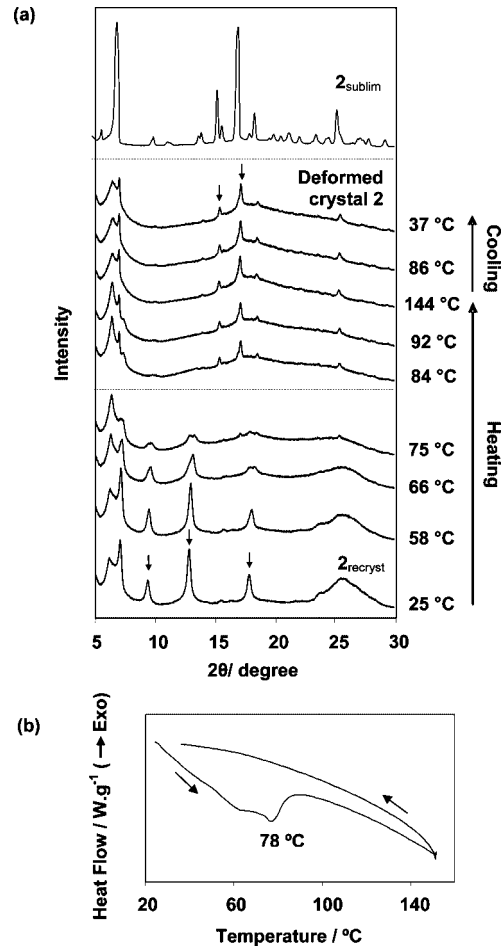

Figure 11. Simultaneous WAXD-DSC of $\mathbf{2}_{\text{recryst}}$: WAXD patterns at various temperatures as compared to that of $\mathbf{2}_{\text{sublim}}$ (a) and DSC thermogram (b).

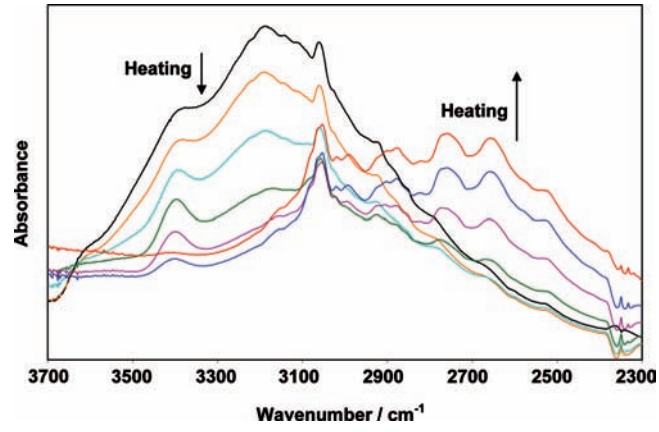

Figure 12. Temperature-dependent FT-IR spectra of $\mathbf{2}_{\text{recryst}}$.

To compare $\mathbf{2}_{\text{recryst}}$ with $\mathbf{2}_{\text{sublim}}$, temperature dependency studies based on WAXD and FT-IR analyses were also applied to $\mathbf{2}_{\text{recryst}}$ (Figures 11 and 12). Figure 11 shows the simultaneous WAXD-DSC measurement results. The WAXD patterns show a little change during 25−75 °C but a drastic change when the temperature reached 84 °C (Figure 11a). At the same time, the DSC thermogram exhibits an endothermic peak at 78 °C, which reflects the evaporation of 2-propanol from the crystals putting in an open pan under the purged dry nitrogen gas stream (Figure 11b). The changes in WAXD patterns and the result obtained from DSC thermogram support each other about the irreversible transition of the packing structure from the solvent-stabilized

SCHEME 3: Temperature Effect on Molecular Packing Structures[a]

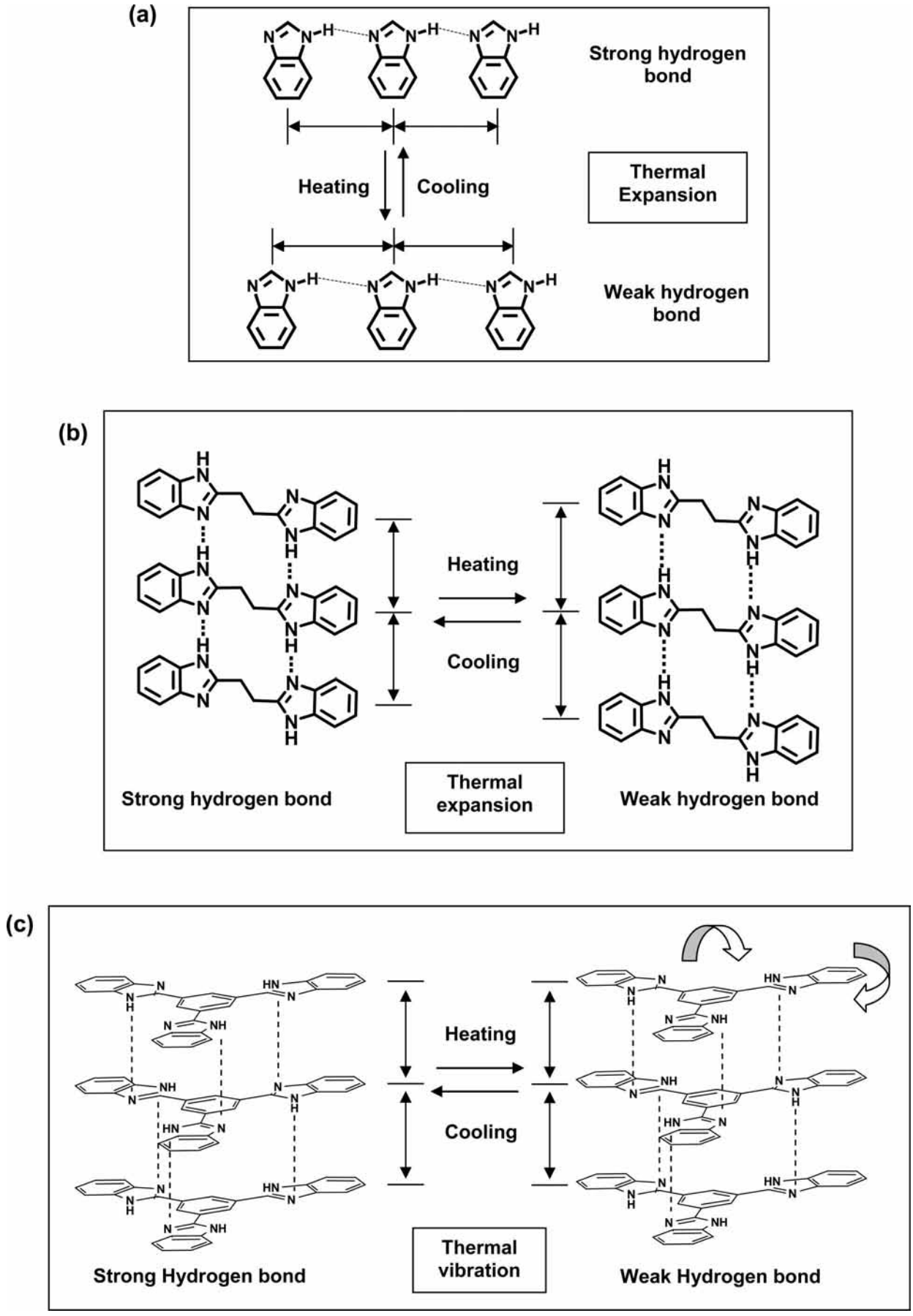

[a] Benzimidazole (a), **1** (b), and **2** (c).

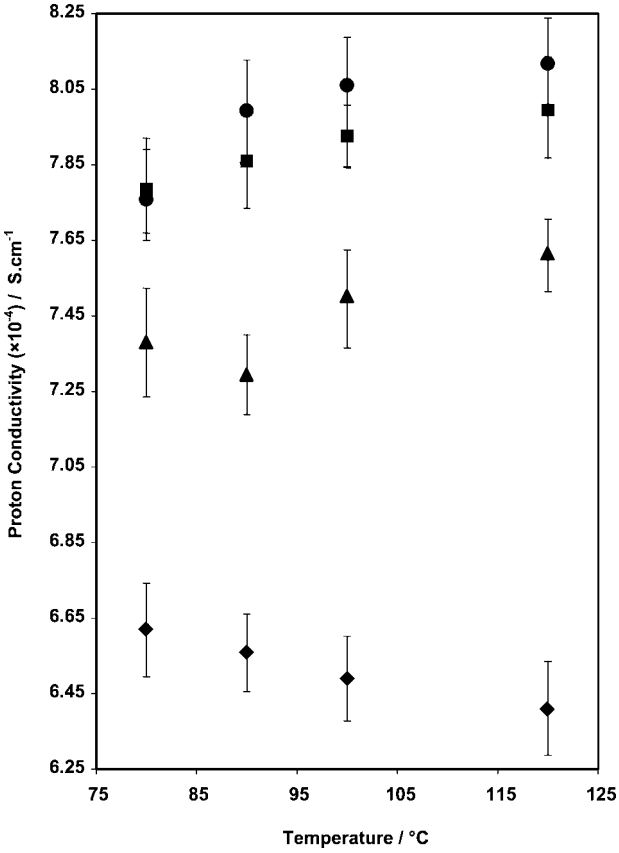

Figure 13. Proton conductivity of the membrane under dry condition: SPEEK (♦), SPEEK-1BI (▲), SPEEK-2BI (■), and SPEEK-3BI (●).

crystal structure ($\mathbf{2}_{recryst}$) to the consequent repacking structure, so-called "deformed crystal **2**" pattern, under the loss of solvent molecules. The packing structure after removing solvent, as seen from the WAXD patterns from 84 to 144 °C and from 144 to 37 °C, is found to be similar to the one observed in $\mathbf{2}_{sublim}$. The FT-IR patterns support the existence of solvent in the crystals. Figure 12 shows the FT-IR spectra of crystal of $\mathbf{2}_{recryst}$ with significant changes of hydrogen bond pattern from O−H type (3600−2500 cm^{-1}) to N−H type (3200−2200 cm^{-1}) when the sample was heated from room temperature to 250 °C. This reflects the change of hydrogen bond pattern from $\mathbf{2}_{recryst}$ to $\mathbf{2}_{sublim}$ by solvent removal. Therefore, the results imply that by simply removing the solvent via heat treatment, we can change both molecular packing structure and hydrogen bond formation of $\mathbf{2}_{recryst}$ to those of $\mathbf{2}_{sublim}$.

Study on Proton Conductivity of Benzimidazole, 1, and 2 Using SPEEK as Polymer Matrices. To evaluate the function of benzimidazole, **1**, and **2** in enhancing proton conductivity, the SPEEK membranes containing benzimidazole, **1**, or $\mathbf{2}_{sublim}$ in an equivalent benzimidazole group (∼15 phr) were prepared. In order to exclude the interference of proton transfer based on a water molecule, all measurements were carried out in dry conditions. Figure 13 shows the proton conductivity of the SPEEK membranes mixed with benzimidazole (SPEEK-1BI), **1** (SPEEK-2BI), and $\mathbf{2}_{sublim}$ (SPEEK-3BI) as compared to the pure SPEEK membrane (SPEEK). For the pure SPEEK membrane, the conductivity is significantly less than those of the blend membranes. In this case, an increase in temperature leads to the decrease in proton conductivity. This might be due to the reduction of membrane humidity when the temperature increased especially above 80 °C. In contrast, the membranes containing the benzimidazole compounds show an increase in proton conductivities when they were heated. This implies that all the benzimidazole compounds (i.e., benzimidazole, **1**, and **2**) function as proton carriers in SPEEK under water-free conditions. It is also clear that an increase in the number of benzimidazole groups on the molecule initiates the effective proton conductivity as seen from the increase in proton conductivity in the order of SPEEK-3BI > SPEEK-2BI > SPEEK-1BI. In other words, this work demonstrates how the intermolecular interaction and packing structure of the compound involves the proton conductivity for the application in the PEMFC.

Conclusion

Di- and trifunctional benzimidazole model compounds, **1** and **2**, were designed and successfully synthesized by a simple reaction between acid chloride and diamine. The comparative studies on molecular packing structure and hydrogen bond formation revealed that **1** and **2** were in well-packed structures with an NH···N intermolecular hydrogen bond network similar to that of benzimidazole. For **2** obtained from recrystallization, X-ray structure analysis illustrated that the crystal structure governed by the molecular complex between one molecule of **2** and six molecules of 2-propanol resulted in the unique structure of solvent-assisted intramolecular hydrogen bonds network. The temperature dependency studies on packing structure and hydrogen bond interaction of a series of mono-, di-, and trifunctional benzimidazole model compounds indicated that the intermolecular interaction is enhanced when the compound is bearing higher number of benzimidazole units with planar shape structure being maintained. Consequently, the stronger molecular packing structure can be achieved and results in the higher resistance of the molecular packing structure on thermal vibrational energy. The improvement in packing structure with the hydrogen bond network obtained from di- and trifunctional benzimidazole favored the proton conductivity as evidenced from the model membranes of SPEEK with benzimidazole, **1**, and **2**.

Acknowledgment. The authors would like to express their gratitude to the Thailand Research Fund (the Royal Golden Jubilee Ph.D. Scholarship, grant no. PHD/0031/2547). The acknowledgement is also to the Thailand Government Research Budget (National Research Council of Thailand), the NRCT-JSPS Joint Research Program (National Research Council of Thailand and Japan Society for Promotion of Science), the Engineering Research and Development Project (National Metal and Materials Technology Center of Thailand), and the Research Task Force Project (Chulalongkorn University) for the research funds and supports. The authors are indebted to JJ-Degussa Chemical (Thailand) Ltd. for PEEK. The appreciation is also to Dr. Suttinun Phongthamrug for crystal analysis.

Supporting Information Available: Crystallographic data (excluding structure factors) for the structures in this paper have been deposited with the Cambridge Crystallographic Data Centre as supplementary publication numbers CCDC 671942 ($\mathbf{2}_{recryst}$) and CCDC 675661 (benzimidazole). Copy of the data can be obtained, free of charge, on application to CCDC, 12 Union Road, Cambridge CB2 1EZ, UK, (fax: +44-1223-336033. E-mail: deposit@ccdc.cam.ac.uk). This material is available free of charge via the Internet at http://pubs.acs.org.

References and Notes

(1) Watanabe, M.; Igarashi, H.; Uchida, H.; Hirasawa, F. *J. Electroanal. Chem.* **1995**, *399*, 239.

(2) Kreuer, K. D. *J. Membr. Sci.* **2001**, *185*, 29.
(3) Alberti, G.; Casciola, M. *Solid State Ionics* **2001**, *145*, 3.
(4) Kreuer, K. D. *Solid State Ionics* **1997**, *94*, 55.
(5) Kreuer, K. D. *Solid State Ionics* **2000**, *136*−*137*, 149.
(6) Yang, C.; Costamagna, P.; Srinivasan, S.; Benziger, J.; Bocarsly, A. B. *J. Power Sources* **2001**, *103*, 1.
(7) (a) Persson, J. C.; Jannasch, P. *Chem. Mater.* **2003**, *15*, 3044–3045. (b) Savadogo, O. *J. Power Sources* **2004**, *127*, 135.
(8) Divisek, J.; Oetjen, H. F.; Peinecke, V.; Schmidt, V. M.; Stimming, U. *Electrochim. Acta* **1998**, *43*, 3811.
(9) Beuscher, U.; Cleghorn, S. J. C.; Johnson, W. B. *Int. J. Energy Res.* **2005**, *29*, 1103.
(10) Jones, D. J.; Rozière, J. *J. Membr. Sci.* **2001**, *185*, 41.
(11) Kreuer, K. D.; Fuchs, A.; Ise, M.; Spaeth, M.; Maier, J. *Electrochim. Acta* **1998**, *43* (10−11), 1281.
(12) Yamada, M.; Honma, I. *Electrochim. Acta* **2003**, *48*, 2411.
(13) Schuster, M. F. H.; Meyer, W. H.; Schuster, M.; Kreuer, K. D. *Chem. Mater.* **2004**, *16*, 329.
(14) Münch, M.; Kreuer, K. D.; Silvestri, W.; Maier, J.; Seifert, G. *Solid State Ionics* **2001**, *145*, 437.
(15) Asensio, J. A.; Gómez-Romero, P. *Fuel Cells* **2005**, *5* (3), 336.
(16) Carollo, A.; Quartarone, E.; Tomasi, C.; Mustarelli, P.; Belotti, F.; Magistris, A.; Maestroni, F.; Parachini, M.; Garlaschelli, L.; Righetti, P. P. *J. Power Sources* **2006**, *160*, 175.
(17) Bozkurt, A.; Meyer, W. H. *Solid State Ionics* **2001**, *138*, 259.
(18) Persson, J. C.; Josefsson, K.; Jannasch, P. *Polymer* **2006**, *47*, 991.
(19) Fu, Y.; Manthiram, A.; Michael, D. G. *Electrochem. Commun.* **2007**, *9*, 905.
(20) Yamada, M.; Honma, I. *Polymer* **2005**, *46*, 2986.
(21) Sun, J.; Jordan, L. R.; Forsyth, M.; MacFarlane, D. R. *Electrochim. Acta* **2001**, *46*, 1703.
(22) Liu, Y. F.; Yu, Q. C.; Wu, Y. H. *Electrochim. Acta* **2007**, *52*, 8133.
(23) Cazacu, A.; Tong, C.; van der Lee, A.; Fyles, T. M.; Barboiu, M. *J. Am. Chem. Soc.* **2006**, *128*, 9541.
(24) Michau, M.; Barboiu, M.; Caraballo, R.; Arnal-Hérault, C.; Perriat, P.; van der Lee, A.; Pasc, A. *Chemistry* **2008**, *14* (6), 1776.
(25) Gaowen, Z.; Zhentao, Z. *J. Membr. Sci.* **2005**, *261*, 107.
(26) Phongtamrug, S.; Tashiro, K.; Miyata, M.; Chirachanchai, S. *J. Phys. Chem. B.* **2006**, *110*, 21365.
(27) Vijayan, N.; Balamurugun, N.; Ramesh Babu, R.; Gopalakrishnan, R.; Ramasmy, P.; Harrison, W. T. A. *J. Cryst. Growth* **2004**, *267*, 218.
(28) Vijayan, N.; Bhagavannarayana, G.; Kanagasekaran, T.; Ramesh Babu, R.; Gopalakrishnan, R.; Ramasmy, P. *Cryst. Res. Technol.* **2006**, *41*, 284.

JP8045774